J Appl Electrochem (2009) 39:1671–1681
DOI 10.1007/s10800-009-9859-5

ORIGINAL PAPER

Electrodeposition and tribocorrosion behaviour of ZrO_2–Ni composite coatings

Lidia Benea

Received: 3 June 2008 / Accepted: 27 February 2009 / Published online: 18 March 2009

Abstract With the objective of producing new functional surfaces with enhanced tribo-corrosion properties we have investigated the electrochemical codeposition of composites in which an electrodeposited metal (nickel) is the matrix and a transition metal oxide (ZrO_2) is the dispersed phase. This paper describes the effect of ZrO_2 dispersed particle codeposition on nickel electrocrystallisation steps as well as the tribocorrosion behaviour of the composite coatings obtained. This system was selected because nickel is an industrially important coating material on steel and other support materials. The cathodic polarization curves have been plotted both in the presence and absence of the insoluble dispersed phase. Electrochemical impedance spectroscopy was used to obtain additional information on the early steps of nickel and nickel matrix composite electrodeposition. Impedance data were acquired with a Solartron type electrochemical interface and frequency response analyzer. A schematic codeposition mechanism is proposed. The influence of zirconium oxide on the nickel electrodeposition steps is discussed. The tribocorrosion properties of ZrO_2–Ni composite coatings (100 μm thickness) have been studied in 0.5 M K_2SO_4 solution on a pin on disc tribo-corrosimeter connected to an electrochemical cell. The normal force applied was 10 N at a rotation speed of 120 rpm. The counterbody (pin) was a corrundum cylinder (7 mm in diameter), mounted vertically on a rotating head, above the specimen. The lower spherical end (radius = 100 mm) of the pin was then applied against the composite surface (disc).

Keywords Composite coatings · Electrodeposition · Co-deposition mechanism · Zirconium oxide · Dispersed phase · Nickel · Tribocorrosion

1 Introduction

Much attention has been attached to the development of ceramic/metal composites because such materials offer outstanding mechanical and multifunctional properties. Composite electroplating is a method of codepositing insoluble particles of metallic or non-metallic compounds with metals or alloys in a plating bath, to improve the material coatings properties such as corrosion resistance, lubrication, hardness or wear-resistance. The coatings thus obtained feature the properties of both metal and dispersed particles and can be considered metal-matrix composites (MMC), obtained through electrodeposition. Composite coatings obtained by metal co-deposition of various dispersed phases during electrocrystallisation have been given special attention in recent years [1–10]. Nickel, copper, chromium, iron, cobalt, silver, gold are mainly used as metal matrix. Metal powders, metal oxides, carbides, borides and polymers were used as co-depositing dispersed particles. Composite coatings are used in both aqueous and high temperature applications. Electric power generation, and waste incineration involve severe conditions and thick coatings have proved effective. Diesel and gas turbine engines undergo high temperature corrosion; therefore highly specialised coatings have been developed. Some

Lidia Benea—ISE Active Member.

L. Benea (✉)
Competences Center Intrfaces-Tribocorrosion-Electrochemical Systems (CC-ITES), Dunărea de Jos University of Galati, 47 Domneasca Street, 800008 Galati, Romania
e-mail: Lidia.Benea@ugal.ro; lidiabd@yahoo.com

nuclear power systems also rely on coatings. Factors that must be taken into account include substrate compatibility, adhesion, porosity, the possibility of repair or recoating, inter-diffusion, the effect of thermal cycling, resistance to wear and corrosion, and last but not least the cost.

In industry, e.g. automotive applications, there is always the risk of materials coming into contact with each other under sliding conditions. In many cases, such industrial components, e.g. bearings, pumps, rolling mill bearings, are required to operate in aqueous environments (corrosive media) where water is either deliberately introduced as a coolant or present as a working fluid. The combined action of wear and corrosion, named tribo-corrosion, often results in a significant increase in the total material loss [11, 12]. This calls for materials having the desired corrosion, friction and wear properties. Accordingly, many efforts have been made to develop materials suitable for aqueous environments.

Ni-based composites, which are in general designed for high temperature applications, possess some extraordinary characteristics such as excellent mechanical properties; good thermal stability, chemical inertness and high wear resistance. The Ni-based composites are successfully used due to their self-lubricating property in a wide temperature range, for instance, the turbine engines used in aviation and electric industries, the radiator sealing systems of the automobile engines, and mechanical devices in atomic reactors. In particular, during recent years, ceramic–Ni composites have been widely investigated as a result of their improved mechanical and tribological properties.

Composite coating materials have been obtained by using dispersed micro sized ZrO_2 particles (mean diameter 10 μm). The influence of ZrO_2 dispersed particles on nickel reduction is discussed. Prior to the wear corrosion tests, the composition and surface morphology of coatings have been investigated by scanning electron microscopy with X-ray analysis (EDS). The presence of particles inside the composite coating was detected by optical microscopy.

The major challenges with the codeposition of the second-phase particles are the achievement of a high level of codeposition and avoiding the agglomeration of particles suspended in the electrolytes. However, there are very few studies on inert particle dispersion in metallic matrices and its influence on mechanical and tribological or tribo-corrosion properties [3, 13]. Zhou et al. [14] discuss the enhanced friction and wear properties of co-deposited Ni–SiC nanocomposite under non-lubricated conditions. Very little information on the tribocorrosion behaviour of composite coatings has been published [15, 16].

The aim of this work is to investigate the influence of ZrO_2 particle dispersion on nickel electro-reduction and on the tribo-corrosion properties of ZrO_2–Ni composite coatings obtained.

2 Experimental

2.1 Preparation of ZrO_2–Ni micro-structured composite coatings

Pure nickel and nickel zirconium oxide codeposition was carried out in common nickel-plating electrolyte with the following composition: 1 M $NiSO_4$—nickel sulphate; 0.1 M $NiCl_2$—nickel chloride; 0.2 M H_3BO_3—boric acid and 1.2×10^{-3} M $[CH_3(CH_2)_{11}OSO_3Na]$—sodium dodecylsulfate. The electrolyte temperature was maintained by water circulation to the thermostated temperature of 45 °C. The electrolyte was prepared from p.a. chemicals and distilled water, which provided the required purity for the potentiodynamic investigations and characterizations of the coatings obtained. Pure dispersed zirconium oxide (ZrO_2) at a concentration of 20 g L^{-1} was suspended in the electrolysis bath. The average particle size was 10 μm. The thickness of the pure nickel and composite deposits was 100 μm and this was verified by measuring the weight before and after deposition, by dissolving the coatings and filtering the particles and also by light microscopy on a cross section. The particles were kept in suspension by magnetic stirring at a rotation rate between 200 and 1,000 rpm. A saturated calomel electrode was used as reference electrode (SCE) in order to determine the influence of the dispersed phase on nickel electrodeposition.

2.2 Structural and chemical analyses

By weighing the electrodes on a microbalance and stripping the deposit we determined the amount of dispersed phase in the composite coatings. The particles were filtered, dried and weighed. The weight percentage of particles in the composite was calculated by the formula:

$$p\% = \frac{m_p}{m_s} 100 \quad (1)$$

where p%—weight percentage of the particles in the composite coating; m_p—particle mass, in grams; m_s—total composite coating mass, in grams.

The uniformity of the dispersed phase distribution in the composite coatings was examined by light microscopy on a cross section. Scanning electron microscopy (SEM) revealed the comparative surface morphology of coatings and the uniformity of zirconium oxide particles in the composite. For tribocorrosion studies the composite coatings were deposited on the top of a cylinder having dimensions: height = 25 and diameter = 25 mm (Fig. 1).

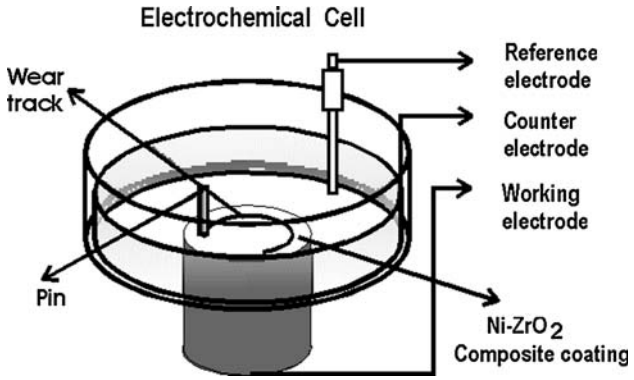

Fig. 1 Schematic set-up for electrochemical measurements during tribocorrosion tests on a working electrode as ZrO_2–Ni composite coating (WE)

2.3 Tribocorrosion studies

In the tribocorrosion studies the electrochemical measurements (open-circuit potential, potentiodynamic polarization) were performed in a three-electrode device with the sample as working electrode, a circular platinum gauze as counter electrode and a Hg/Hg_2SO_4/saturated K_2SO_4 solution as reference electrode (SSE = + 670 mV vs. NHE),(see Fig. 1). The electrodes were connected to a PAR273A potentiostat controlled through a computer by using Corrware 2.2 (Scribner) software.

The tribocorrosion properties were studied in the following conditions:

Solution: 0.5 M K_2SO_4;
Tribo corrosimeter: pin on a disc connected to the electrochemical cell;
Normal Force: 10 N;
Rotation Speed: 120 rotations min^{-1}.

The samples were installed in the electrochemical cell containing the electrolyte and electrodes and mounted on a pin-on-disc tribometer with the working surface of the specimen facing upwards.

The counterbody (pin) was a corrundum cylinder (7 mm in diameter), mounted vertically on a rotating head above the specimen. The lower spherical end (radius = 100 mm) of the pin was then applied against the composite surface (disc) with a normal force of 10 N. When rotation was applied, the end of the pin draws a circular wear track (16 mm in diameter) on the working composite surface (Fig. 1).

Continuous friction tests were carried out at 120 rpm (sliding speed 100 mm s^{-1}) under 10 N (average pressure 120 MPa for Hertzian contact conditions). This mechanical load was repeated over 2,500 cycles (10,000 complete rotations of the pin on the coating surface). Some features of these tests reproduce the wear conditions of composite coatings in practical use. 0.5 M K_2SO_4 was used as corrosive and passivating electrolyte for the tribocorrosion tests.

After the tests had been carried out, the sample surfaces were analysed by SEM and EDS.

Local wear in the wear track was also measured. From the wear track recorded with an optical high resolution microtopograph, with a lateral resolution of 1 μm and a vertical resolution of 30 nm, the volume of the wear track was measured and the corresponding weight loss was calculated.

3 Results and discussion

3.1 Influence of dispersed ZrO_2 micro-particles on nickel ellectrocrystallisation

Cathodic polarization curves and electrochemical impedance spectroscopy diagrams performed at cathodic potentials were used to study the influence of zirconium oxide as dispersed particles on the mechanism of nickel electrocrystallisation.

3.1.1 Cathodic polarization curves

The influence of the dispersed phase on the nickel electrodeposition was observed on cathodic polarization curves plotted with and without dispersed phase. No such measurements could be found in the literature for the purposes of comparison; thus the interpretations of our polarization curves have been based on existing theories of metal and alloy electrocrystallisation [17–19]. From the analysis of cathodic polarization curves in the presence and absence of dispersed zirconium oxide the following remarks can be made:

- Dispersed zirconium oxide phase does not alter the shape of the cathodic polarization curves during nickel electroplating. These curves are only slightly shifted to lower values of the metal reducing voltage (see Fig. 2).
- Zirconium oxide as dispersed phase in the nickel electrolyte does not change the electrocrystallization mechanism of nickel, but it does take part in the process by increasing the metal deposition rate, acting as a catalytic factor. For example at the same current density metal ion reduction over-voltage is lower in the presence of zirconium oxide in the electrolyte, as shown on curve [b] from Fig. 2.
- The larger amount of metal being deposited in the presence of zirconium oxide as dispersed phase may be due to the active species, which are adsorbed or formed on the particle surfaces to be subsequently reduced on the cathode surface.

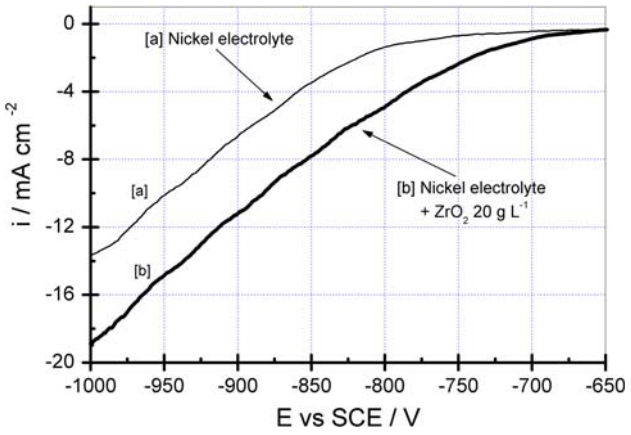

Fig. 2 Cathodic polarization curves performed with and without dispersed ZrO_2 particles in the nickel electrolyte: (a) pure nickel-plating electrolyte; (b) nickel-plating electrolyte with 20 g L^{-1} zirconium oxide

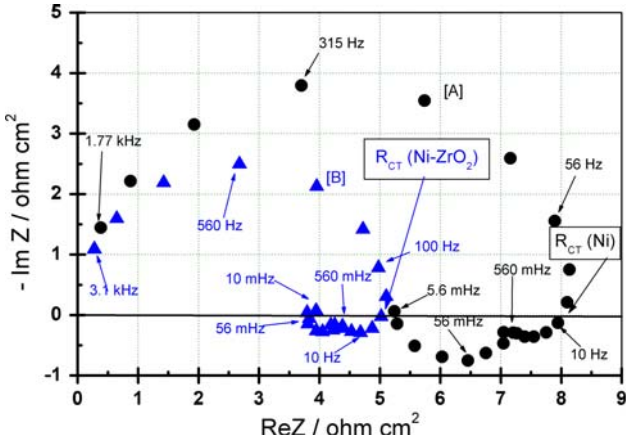

Fig. 3 Complex plane representation of the impedance diagrams at the same cathodic reducing overpotential of −1,150 mV versus saturated calomel electrode (SCE): (a)—*solid up-triangles*: pure nickel electrodeposition (b) *solid circles*—composite coating co-deposition with ZrO_2 dispersed particles in the nickel matrix

– On the growing coating, which is the result of competition between the nucleation steps and crystal growth the zirconium oxide acts as a catalyst for metal ion reduction leading to an increase in the number of active nucleation sites.
– As is well known, an increase in the current density leads to an increase in the number of nucleation sites so that the crystal size becomes smaller within the electrodeposited metal structure. At the same current density the effect of the oxide involved in electrochemical nickel deposition induces the same growth of the active nucleation sites. This conclusion further suggests that the oxide involved in the metal deposition will change in structure. The modification of crystallite size during composite ZrO_2–Ni electrodeposition was checked by investigating the surfaces with respect to the pure nickel electrodeposited at the same current density by means of scanning electron microscopy. The decrease in crystallite size will have a different influence on the reactivity of the composite surface compared with pure nickel.

3.1.2 Impedance diagrams during electrodeposition

Electrochemical impedance spectroscopy (EIS) was used to obtain additional information on the early steps of nickel deposition and the influence of dispersed particles.

Electrodepositions of pure nickel and nickel in the presence of zirconium oxide have were carried out at the same cathodic overpotential of −1,150 mV versus SCE (saturated calomel electrode). For the same cathode surface, the current density was 10 mA cm^{-2} in the case of pure nickel electrodeposition and it subsequently increased to 17.4 mA cm^{-2} in the presence of zirconium oxide particles in the electrolyte. There is good agreement with the cathodic polarization diagrams showing an increase in deposition current at the same cathodic potential. The complex plane impedance diagrams for pure nickel and nickel matrix with zirconium oxide composite coatings are illustrated in Fig. 3. The shape of the diagram in the presence of oxide particles is changed in the low frequency range only and the charge transfer resistance is lower. Fitting the diagram with a simple equivalent circuit (the semicircle) gave the charge transfer resistance values (Table 1).

In Fig. 4A and B the capacitance (C_p) and conductance ($1/R_p$) curves versus logarithm of frequency corresponding to Nyquist representations of impedance diagrams plotted are presented. Solid circles and solid squares on both diagrams represent the negative values of capacitance versus log frequency. The impedance diagrams for the pure nickel and ZrO_2–Ni composite electrodeposition have the same shape; this means that the time constants for the intermediate steps have the same values. This confirms that dispersed particles do not modify the metal electrocrystallisation mechanism; they only activate the charge transfer process.

Table 1 shows the values of charge transfer resistance and double layer capacitance calculated from impedance measurements. The charge transfer resistance is smaller in

Table 1 Impedance data calculated from the diagrams plotted for pure nickel and zirconium oxide composite coatings

Calculated data	Type of coating	
	Pure Ni	ZrO_2–Ni composite coating
Double layer capacitance C_{dl} (μFcm^{-2})	59	53
Charge transfer resistance R_{CT} (ohm cm^2)	8	5

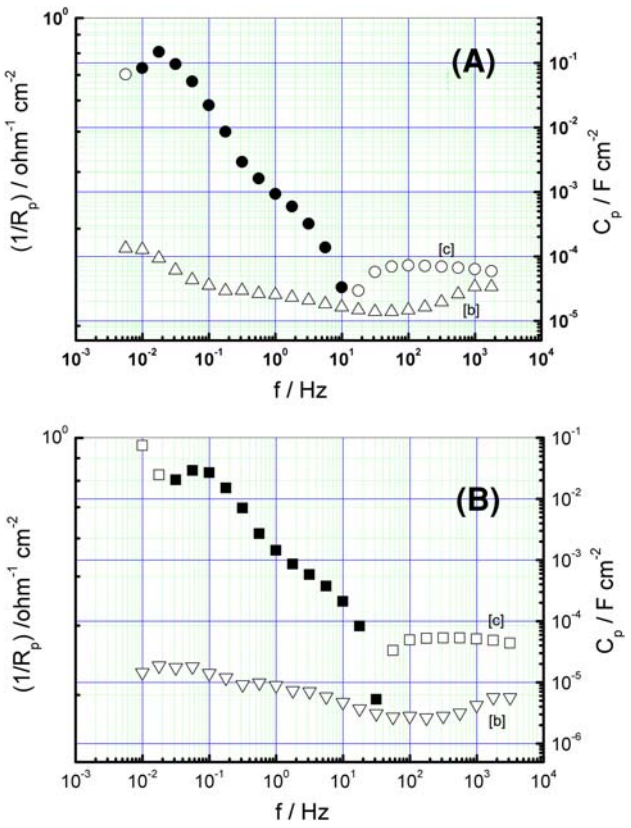

Fig. 4 **A** Impedance data for ZrO_2–Ni composite coating electrodeposition represented as capacitance and conductance: [b] (*up-triangle*) 1/Rp versus log frequency; [c] (*open* and *solid circle*) Cp versus log frequency. *Solid circles* indicate the negative values of capacitance. **B** Impedance data for pure Ni electrodeposition represented as capacitance and conductance: [**b**]—(*down triangle*) 1/Rp versus log frequency; [c]—(*open* and *solid square*) Cp versus log frequency. *Solid squares* represent the negative values of capacitance

the case of zirconium oxide co-deposition, having the value of $R_{CT} = 5$ ohm cm^2 and higher for pure nickel electroplating, $R_{CT} = 8$ ohm cm^2 respectively.

Nickel electrodeposition is strongly influenced by hydrogen discharge and can take place according to the following intermediate steps (Epelboin et al. and Chassaing et al. [20, 21]).

$$Ni^{2+} + e \rightarrow Ni^{+}_{ads} \quad (2a)$$

$$Ni^{+}_{ads} + e \rightarrow Ni \quad (2b)$$

$$Ni^{2+} + Ni^{+}_{ads} + 2e \rightarrow Ni + Ni^{+}_{ads} \quad (2c)$$

$$2(H^{+} + e) \rightarrow H_2 \quad (2d)$$

It can be considered that by decreasing the charge transfer resistance, the ZrO_2 particles activate the nickel ion reduction. The surface-active species are the adions Ni^{+}_{ads}, more or less solvated or complex. $NiOH_{ads}$ is proposed as intermediate species in the nickel dissolution and deposition mechanism.

Hydrogen adsorption and inclusion into the deposit inhibits hydrogen development according to the reaction (2d). The influence of zirconium oxide particles on the cathodic polarization curves (Fig. 2) and impedance diagrams (Fig. 3) reveals the activation effect of the nickel ion reducing reaction (steps 2a and 2b). The reduction of hydrogen ions can also be considered as an activated step (reaction 2d).

During the electrochemical co-deposition the zirconium oxide particles catalyze the adsorbed intermediate step according to reaction (2a), thus decreasing the influence of charge transfer for the final reaction (2b). This can be easily observed on the impedance diagrams plotted in the complex plane (Fig. 3) and in Table 1.

In the Ebelboin mechanism we consider that the preferentially catalyzing intermediate step is $Ni^{+}_{(ads)}$. It is well known that electrodeposition is a competition between nucleation and crystal growth. Nucleation and growth are in competition to determine the grain size [22].The grain size of electrodeposited nickel can be reduced using additives in the nickel bath [22]. The micro sized ZrO_2 particles act as nucleation sites to the detriment of crystal growth. The corresponding nickel matrix has smaller crystal size according to this mechanism. In further SEM surface morphology investigations we observed surface changes of the composite as compared with the pure nickel coating, to smaller grain sizes. In general, the co-deposition mechanism is still not clear and further studies will have to address the details of the process.

3.2 Structural aspects of ZrO_2–Ni composite coatings

SEM Micrographs (surface) of the coatings obtained by electrodeposition show comparison between a pure nickel coating (Fig. 5) and nickel with zirconium oxide composite

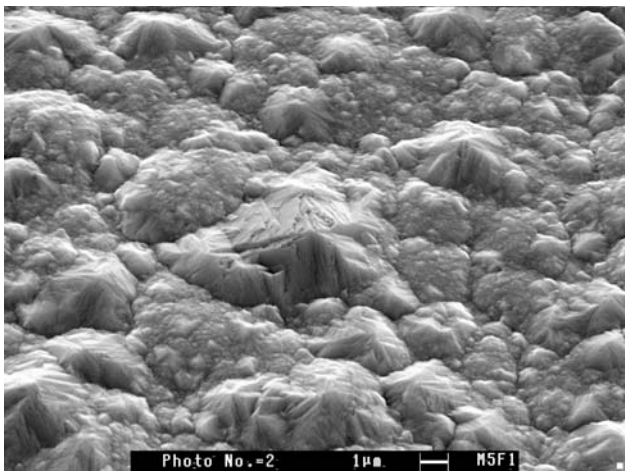

Fig. 5 SEM micrograph of pure nickel coating surface morphology

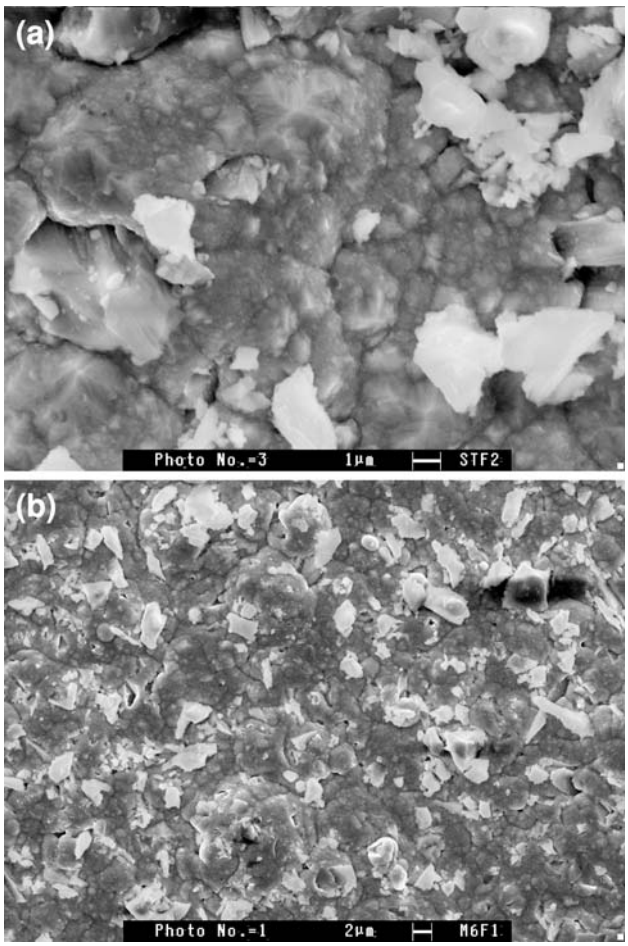

Fig. 6 (**a**, **b**) SEM micrograph of ZrO_2–Ni dispersion coating surface morphology

coatings (Fig. 6a, b) carried out with 20 g L^{-1} of ZrO_2 in the plating bath.

The pure nickel deposit has a rather regular surface, whereas the composite coating develops a nodular disturbed surface structure. The zirconium oxide particles are clearly visible on the surface with a homogeneous distribution (white particles) in Fig. 6a, b. The X-ray disperse energy analysis revealed spectra not only with zirconium but also with nickel. This suggests that particles are not free on the coating surface but have a thin layer of nickel. The nickel layer can be accounted for from the reduced nickel ions at the cathode.

The surface analysis of composite coatings is not the most suitable method to determine the presence of zirconium oxide in the nickel matrix, but it is appropriate to observe the morphology and surface structure changes. One of the most reliable methods to observe the distribution of ZrO_2 particles in the nickel matrix consists in studying the cross section of a deposit. The optical microstructure shows the presence and distribution of zirconium oxide particles (8 mass%) in the nickel matrix

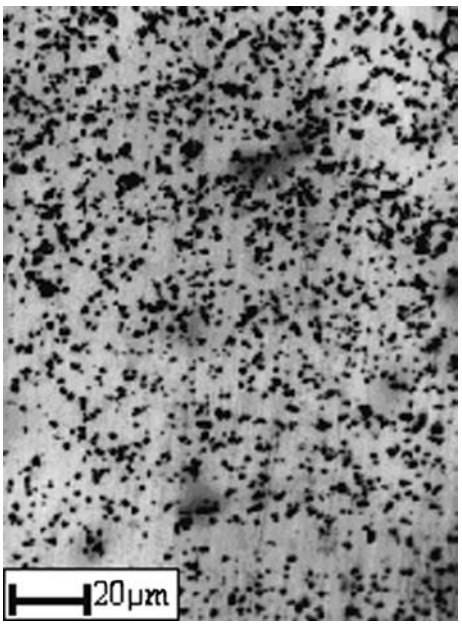

Fig. 7 Optic microstructure of ZrO_2–Ni composite coatings with 8% ZrO_2. Cross section of the coating

(Fig. 7). On the optical micrograph ZrO_2 particles are uniformly distributed within the composite coating (zirconium oxide appears as black points). The more accurate content of dispersed particles in the composite coating was determined by the method described in Sect. 2.2.

The corrosion and tribocorrosion properties of composite coatings are improved in comparison with pure nickel coatings.

3.3 Microhardness of ZrO_2–Ni composite coatings

The microhardness of pure Ni and ZrO_2–Ni composite coatings was determined by optical microscopy using a Microhardness Tester AT201. Vickers microhardness data on zirconium oxide composite coatings compared to pure nickel coatings are presented in Fig. 8. The values reported in Fig. 8 were obtained by means of the last three indentations performed in different positions on the coating surface using a load of 200 g for pure nickel coating and 300 g for composite coatings.

The increase in the microhardness of ZrO_2–Ni dispersion coatings is due to ZrO_2 particle incorporation in the nickel matrix and changes in the microstructure and grain size. The microhardness of ZrO_2–Ni composite coatings also depends on the particle content in the nickel matrix as shown in Fig. 8 for two different percentages of dispersed ZrO_2 particles. Improvement in microhardness of composite coatings compared with pure metal coatings has also been reported elsewhere [14, 23]. The values of microhardness of ZrO_2–Ni composite coatings are close to those of hard chromium coatings [24].

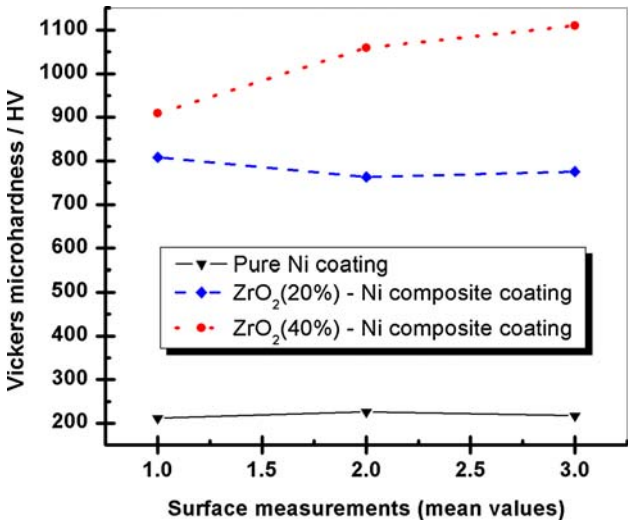

Fig. 8 Results of Vickers microhardness testing on pure nickel and ZrO_2–Ni composite coatings with ZrO_2

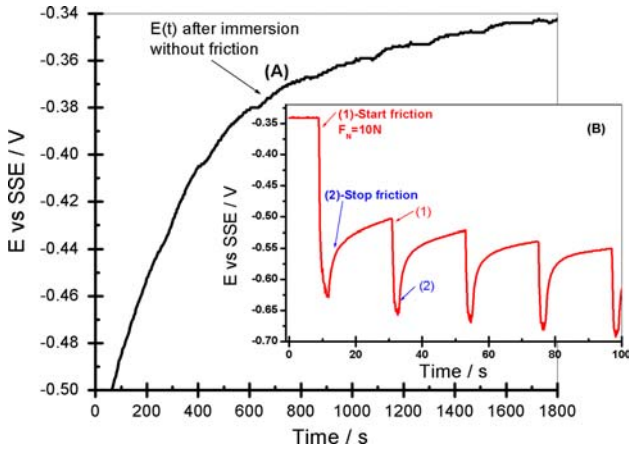

Fig. 9 Variation of the open circuit potential of ZrO_2–Ni composite coating immersed in 0.5 M K_2SO_4: Layer a after immersion in solution indicating the passive state of the surface; Layer b step (1)—after loading a normal force of 10 N; step (2)—after stopping the friction

3.4 Tribocorrosion studies

3.4.1 Open circuit potential measurements

The open circuit potential recorded during uni-directional pin-on-disc sliding tests, in which the disc is the material under investigation, is a mixed potential reflecting the combined state of the unworn disc material and the material in the wear track. A galvanic connection between worn and unworn parts on the disc surface is possible [23, 25, 26]. Consequently, the open circuit potential depends on the following parameters:

- The respective intrinsic open circuit potentials of the materials in worn and unworn areas. These open circuit potentials are different because the electrochemical state of the metal is disturbed by the removal of the surface films that may consist of adsorbed species, passive films, or corrosion products, in the sliding contact, and by mechanical straining of the metal.
- The ratio of worn to unworn areas. In particular, if the extent of the worn area increases, the open circuit potential of the disc will shift depending on the controlling electrochemical processes, being either the anodic (e.g. the dissolution of the metal matrix) or the cathodic reaction (e.g. the reduction of hydrogen or dissolved oxygen).
- The relative position of worn and unworn areas. As a result of the galvanic coupling, a current flows between anodic and cathodic areas. The ohmic drop may induce a non-uniform distribution of potential and current density over the disc surface.
- The measured open circuit potential is thus an average value depending on that distribution,

  The mechanism and kinetics of the anodic and cathodic reactions in worn and unworn areas.

The evolution of the open circuit potential is shown in Fig. 9. The evolution of the open circuit potential was measured under unloaded (Fig. 9 layer A) and mechanically loaded conditions (Fig. 9 layer B).

After immersion in the test solution the open circuit potential tends slowly to a more positive value indicating passivation of the ZrO_2–Ni composite surface, (Fig. 9 layer A). By imposing a normal loading force of 10 N the open circuit potential is moves to more active values, (Fig. 9 layer B—step (1)).

When friction is stopped (step 2 in Fig. 9 layer B), competition between repassivation and dissolution occurs. At the end of the periods of friction, when friction is stopped, the increase in E_{OC} indicates the restoration of the passive film on the areas where it was removed by friction.

3.4.2 Polarization diagrams

The polarization curves of ZrO_2–Ni composite coatings in 0.5 M K_2SO_4 were recorded under continuous friction (10 N; 120 rpm), and without applied load, by direct potentiodynamic scan from the hydrogen evolution potential domain up to the beginning of the transpassive dissolution domain. These curves are presented in Fig. 10.

If the composite surface of the sample is not subjected to rubbing, Fig. 10 curve (1) hydrogen evolution and oxygen reduction are the only reactions detected in the potential domain A. In domain B and C, the composite surface is passivated, the current remaining very small and the zero-current potential lying between −0.8 and −0.6 V versus SSE.

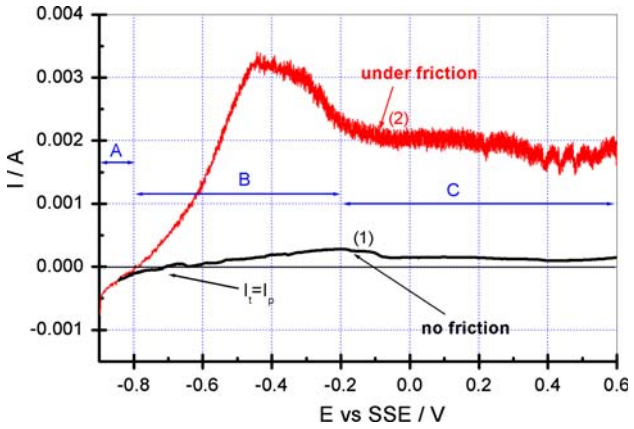

Fig. 10 Potentiodynamic polarization curves of ZrO_2–Ni composite coating immersed in 0.5 M K_2SO_4 recorded by direct potential scan at 0.1 V min^{-1}: (1) no friction applied; (2) continuous friction (10 N and 120 rpm)

When friction is applied, Fig. 10 curve (2) the shape of the polarization diagram changes: hydrogen evolution on the composite surface is not modified in domain A, but an anodic current of about 3 mA appears in the potential range from −0.5 to −0.3 V versus SSE, indicating dissolution of the coating. A first approach for interpreting the polarization curve under friction can be developed based on the concept of "*active wear track*" [22].

The measured current can be considered as the sum of two partial currents I_t and I_p ($I = I_t + I_p$). I_t is the current originated in the wear track areas where the passive film is destroyed and the metal is active, and I_p the current linked to the surface is not subjected to friction and remains in passive state.

- At the zero-current potential where $I = 0$, galvanic coupling is established. I_t and I_p are different from zero, and $I_p = -I_t$. These partial currents flow between the active wear track areas and the rest of the surface. On the wear track, where dissolution of the material and the formation of a new passive film occurs, I_t is anodic. On the remaining surface, I_p is cathodic and is related to reactions such as dissolved oxygen reduction or hydrogen reduction.
- When the potential increases, the galvanic coupling is broken and I_t is no longer equal to $-I_p$. Both I_t and I_p increase. As a result, the measured current I, flowing between the specimen and the counter electrode increases. On the surface not subjected to friction and in the passive state, I_p cannot exceed the value of the current measured at the same potential on the unrubbed specimen. By comparing the values of I in both conditions (see Fig. 10), it can be deduced that, under friction, $I = I_t$ (from −0.78 to 0.6 V versus SSE). The total current measured under friction, and its evolution with applied potential, are characteristic of the behaviour of a composite surface in the wear track. The steep increase in current with potential around the zero-current potential indicates that rapid dissolution occurs in the wear track.
- The further decrease in dissolution current above −0.3 V versus SSE reveals the effect of repassivation in the active wear track. The rate of this reaction, occurring in the areas where the passive film is removed, increases with potential. This induces a decrease in the total depassivated area, resulting in lower dissolution current.

Thus, polarization curves reveal the occurrence of depassivation and dissolution of the composite surface induced by friction in the wear track, and gives the opportunity of quantitative measurements concerning the variation of the active wear track area with tribological parameters (normal load, sliding speed, etc.).

The depassivation of these areas along the wear track was interpreted as the result of the potential distribution generated over the surface of the specimen by the galvanic coupling between the anodic active wear track areas (having low specific corrosion potential) and the cathodic passivated surrounding surface (having higher specific rest potential).

3.4.3 *SEM surface morphology after continuous friction*

After tribocorrosion tests the surface of samples was analysed by SEM and EDS systems. Figure 11a, b shows SEM micrographs of the wear track after continuous friction (10,000 complete rotations of the pin on the coating surface). The EDS system was used in order to compare the surfaces on the wear track area and near the wear track area (where the surface was not subject to friction).

The chemical analysis after tribocorrosion tests on continuous friction (FC) highlighted a different content of zirconium particles on the near area of the wear track compared with the wear track area. On the unrubbed surface the content of zirconium oxide was 13.07% (mass percent) whereas inside of the track surface area was around 22.18%. This suggests that during the friction process, the co-deposited ZrO_2 particles gradually protruded out of the matrix, which carried the load transferred from the matrix; as a result the amount of plastic deformation and wear were reduced.

The mechanical damage of the sample surfaces induces activation of the metal structure, which is well described by the corrosion potential. However, the trend with time shows a further increase in the corrosion potential towards higher values. The equilibrium between the mechanical damage and the electrochemical processes at the metal

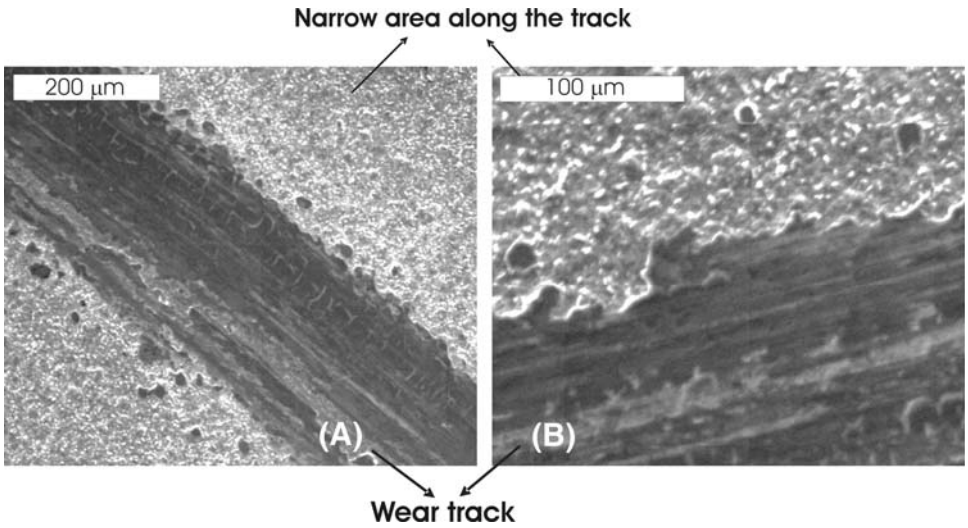

Fig. 11 SEM micrographs of ZrO_2–Ni composite surface after continuous friction tests (FC) of 10,000 complete rotations of pin on coating surface

surface needs some time to be reached. Initially the mechanical wear induces a rapid deterioration of the protective surface layers, which causes a drastic decrease in corrosion potential.

3.4.4 Microtopographic survey of the worn surface

Local wear in the wear track was also measured. It was deduced from surveys of the wear track recorded with an optical high-resolution microtopograph with a lateral resolution of 1 µm and a vertical resolution of 30 nm: the volume of the wear track was measured and the corresponding weight loss was calculated. Figure 12 presents a 3D surface measured after a continuous friction test on ZrO_2–Ni composite coating.

After data processing to eliminate roughness the wear loss was calculated and transformed into weight loss depending on tribocorrosion parameters.

When a tribo-element is made of a ductile element such as Al, Cu, Ni, Fe or an alloy with a combination of such materials, material in the contact region undergoes severe plastic deformation under the combined stresses of compression and shear. Large plastic deformation generally introduces large wear rate since the wear surface tends to become rough and protective surface layers are easily destroyed. Scar surface profiles of pure Ni coating show higher debris and higher roughness parameters [15].

Surface roughness parameters in the middle of the wear track (mean value) [15] are: $R_a = 8.19$ µm; $R_q = 9.67$ µm; $R_p = 28.50$ µm; $R_v = 29.50$ µm for pure nickel coating. In the case of ZrO_2–Ni composite surface these values were under 1 micron. The introduction of a harder reinforcing phase in the ductile matrix by a certain volume fraction can reduce ductility of the matrix material in the contact region and wear of the matrix can be reduced as a result.

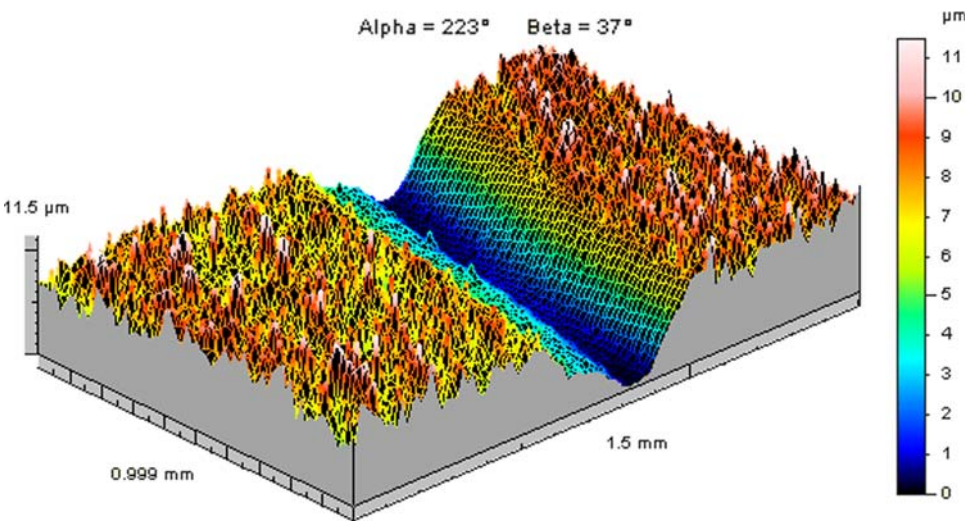

Fig. 12 3D—microtopographic image of wear track area after continuous friction on ZrO_2–Ni composite coating

The dispersed ZrO_2 microparticles in the nickel coatings improve wear and corrosion resistance. The summary results obtained after continuous friction of ZrO_2–Ni composite coatings show a wear-corrosion rate value of 18 g km^{-1} being smaller than the previous results obtained for pure nickel coating [15] with a wear corrosion rate value of 54 g km^{-1}.

The introduction of a harder reinforcing phase in the ductile matrix by a certain volume fraction can reduce ductility of the matrix material in the contact region and wear of the matrix can be consequently reduced.

From the above results, the incorporation of ZrO_2 micro dispersed particles improves the tribocorrosion performance of ZrO_2–Ni composite coatings. Strengthening is achieved because dispersed particles restrain matrix deformation by mechanical constraint. Thus for the ZrO_2–Ni composite coating, the enhancement of hardness is also related to the dispersion-strengthening effect caused by ZrO_2 particles in the composite coatings, which impede the motion of dislocations in the metallic matrix [14].

4 Conclusions

The experiments have shown the possibility of obtaining composite coatings having a nickel matrix by metal electrodeposition with inert particles of zirconium oxide, featuring different effects in the intermediate steps of electrocrystallisation which cause different structures and properties of the coatings obtained.

The pure nickel deposit has a regular surface. On the other hand the surface of composite coating presents different morphology with smaller nodule like grains. The morphology of composite coatings is uniform and the zirconium oxide particles are definitely visible on the surface but with a thin layer of nickel on them.

The zirconium oxide acts as a catalyst for nickel ion reduction, resulting in more nucleation sites. It can therefore be concluded that metal electro-deposition from electrolyte solutions is activated by means of the electrically active ions adsorbed on the ZrO_2 oxide surface. Zirconium oxide dispersed in the nickel deposition electrolyte does not change the electro-crystallisation mechanism of nickel but takes part in the process by increasing the metal deposition rate. For the same current density, the metal ion reduction overvoltage is lower in the presence of zirconium oxide particles in the electrolyte.

ZrO_2 micro dispersed particles co-deposited with nickel induce structural modifications of the metallic nickel matrix to lower and finer grain sizes, which also modifies the properties of the composite coatings obtained.

The tribocorrosion behaviour of ZrO_2–Ni microstructured composite coatings in a pin on disc sliding system in 0.5 M K_2SO_4 solution was investigated combined with in situ electrochemical (potential and polarization diagrams) measurements and ex-situ SEM–EDS and micro-topographic surveys.

This work points to the capabilities of electrochemical methods such as open circuit potential measurements, polarization curve measurement, for the in situ investigation of materials used under tribocorrosive conditions in sliding contacts. They can provide essential information, not only on the surface conditions of composite surface in sliding contacts, but also on the kinetics of reactions that control the corrosion component in the material loss during tribocorrosion tests.

The zirconium oxide–nickel composite coating is affected by a tribocorrosion process when subject to friction in 0.5 M K_2SO_4. This tribocorrosion process involves mechanical destruction of the passive film on the contact areas by friction and subsequent restoration of the film (repassivation) when friction stops.

The tribocorrosion properties of ZrO_2–Ni composite coatings are improved due to dispersed ZrO_2 particle incorporation in the nickel matrix followed by structural modification and an induced dispersion-strengthening effect.

Acknowledgements We thank COST-D33—Chemistry-STSM and CNCSIS National Grant 1347 for financial support.

References

1. Guglielmi N (1972) J Electrochem Soc 119(8):1009
2. Benea L, Bonora BL, Borello A, Martelli S, Wenger F, Ponthiaux P, Galland J (2001) J Electrochem Soc 148(7):C461
3. Benea L, Bonora PL, Borello A, Martelli S (2002) Mater Corros 53:23
4. Benea L, Bonora PL, Wenger F, Ponthiaux P, Galland J (2002) Processing and properties of electrodeposited composite coatings—results and perspectives, CD-ROM proceeding of 15th international corrosion congress—frontiers in corrosion science and technology Granada Spain, 22–27 September
5. Benea L (1998) Composite electrodeposition—theory and practice. Ed Porto Franco, RO, 187 pp
6. Watson SW (1993) J Electrochem Soc 140:2235
7. Maurin G, Lavanant A (1995) J Appl Electrochem 25:1113
8. Fransaer J, Celis JP, Roos JR (1992) J Electrochem Soc 139:413
9. Fransaer J, Celis JP, Roos JR (1993) Metal Finish 91:97
10. Ciubotariu AC, Benea L, Lakatos-Varsanyi M, Dragan V (2008) Electrochim Acta 53:4557
11. Garcia J, Conde A, Langelaan G, Fransaer J, Celis JP (2003) Corros Sci 45:1173
12. Cattarin S, Musiani M (2007) Electrochim Acta 52:2796
13. Hou KH, Ger MD, Wang LM, Ke ST (2007) Wear 253:994
14. Zhou Y, Zhang H, Qian B (2007) Appl Surf Sci 253(20):8335
15. Benea L, Bonora PL, Borello A, Martelli S (2001) Wear 249 (10–11):995
16. Bratu F, Benea L, Celis JP (2007) Surf Coat Technol 201 (16–17):6940
17. Erdey-Grúz T (1972) Kinetics of electrode processes. Ed Akadémiai Kiadó, Budapest, HU, p 350

18. Radovici O (1986) Tratat de Chimie Fizică. Electrochimie Ed. Academy, Bucharest, RO
19. Bockris JO'M (1967) Fundamental aspects of electrocrystallization. Plenum Press, NY
20. Epelboin I, Joussellin M, Wiart R (1981) J Electroanal Chem 119:61
21. Chassaing E, Joussellin M, Wiart R (1983) J Electroanal Chem 157:75
22. Moti E, Shariat MH, Bahroloom ME (2008) J Appl Electrochem 38:605
23. Garcia J, Drees D, Celis JP (2001) Wear 249:452
24. Fontanesi C, Ciovanardi R, Cannio M (2008) J Appl Electrochem 38:425
25. Oltra R (1991) In: Sagües AA, Meletis EI (eds) Wear-corrosion interactions in liquid media. Minerals Metals and Materials Society, Warrendale, p 3
26. Benea L, Ponthiaux P, Wenger F, Galland J, Hertz D, Malo JY (2004) Wear 256(9–10):948